Chapter 5

Environment-Friendly Approach in the Synthesis of Metal/Polymeric Nanocomposite Particles and Their Catalytic Activities on the Reduction of *p*-Nitrophenol to *p*-Aminophenol

Noel Peter Bengzon Tan and Cheng Hao Lee

Additional information is available at the end of the chapter

http://dx.doi.org/10.5772/intechopen.68388

Abstract

In this chapter, an environment-friendly approach in synthesizing Au and Au@Ag metal nanoparticles using a microgel is demonstrated. Poly(*N*-isopropyl acrylamide)/polyethyleneimine microgel was used as a multifunctional template to reduce metal ions to metal nanoparticles, stabilize and immobilize these metal nanoparticles, and regulate their accessibility within the template. Such multifunctional roles of microgel template were possible due to their unique properties (i.e., amino groups reducing capability, electrostatic and steric stabilizing properties, and swelling/deswelling properties). Characterizations of these metal/polymeric composite particles were also performed, such as scanning electron microscope (SEM), transmission electron microscope (TEM), Zeta-potential, UV-vis spectroscopy, X-ray Diffraction (XRD), and X-ray photoelectron spectroscopy (XPS). To test the catalytic activities of both gold and gold@silver nanoparticles in the microgel template, a model reaction (i.e., reduction of *p*-nitrophenol to *p*-aminophenol) was performed. Results showed that bimetallic gold@silver gave 10 times higher catalytic activity compared to monometallic gold nanoparticles. With the simple one-step synthesis, a highly scalable process is possible.

Keywords: green synthesis, gold nanoparticles, Au@Ag bimetallic nanoparticles, core-shell particles, smart microgel particles, smart materials

1. Introduction to metal/polymeric nanocomposite particles

Metal/polymeric nanocomposite particles are a combination of both metal particles and polymers in nanoscale. They come in different terms and play of words. But simply they are

colloidal polymers with metal nanoparticles. Metal nanoparticles that can be incorporated into different colloidal polymeric systems are magnetic, semiconductor, and noble metals. On the other hand, colloidal polymers act as carriers of these metal nanoparticles. They are mostly referred to as polymer templates. These templates can either be soluble (i.e., colloidally soluble) or insoluble (i.e., solid or heterogeneous) polymers. **Figure 1** displays the different conformations of metal nanoparticles with polymeric templates. For example, metal nanoparticles are seen as core (**Figure 1a** and **b** [1–2]) or part of the polymeric template shell (**Figure 1c** [3]) or attached to both the core and shell of the composite (**Figure 1d** [4]).

Applications of metal/polymeric nanocomposites vary from the fields of chemistry (e.g., catalysis, sensors, and polymers), physics (e.g., optics and electronics), biology (e.g., detection and control of microorganism), and nanomedicine (e.g., drug development and immunoassay).

There are two general approaches in synthesizing metal nanoparticles: top-down and bottom-up. Top-down methods comprise physical methods such as lithography and etching of bulk metals to nanoscopic scale. Bottom-up approaches are more common these days than the top-down. The bottom-up approach also has an advantage of generating uniform nanoparticles with controlled size and shape.

Bottom-up approaches or commonly referred to as wet chemical methods were pioneered for more than a century ago [5]. In particular, Michael Faraday's method used metal-salt solution mixed with reducing agents (e.g., hydrogen, alcohol, hydrazine, or borohydride)

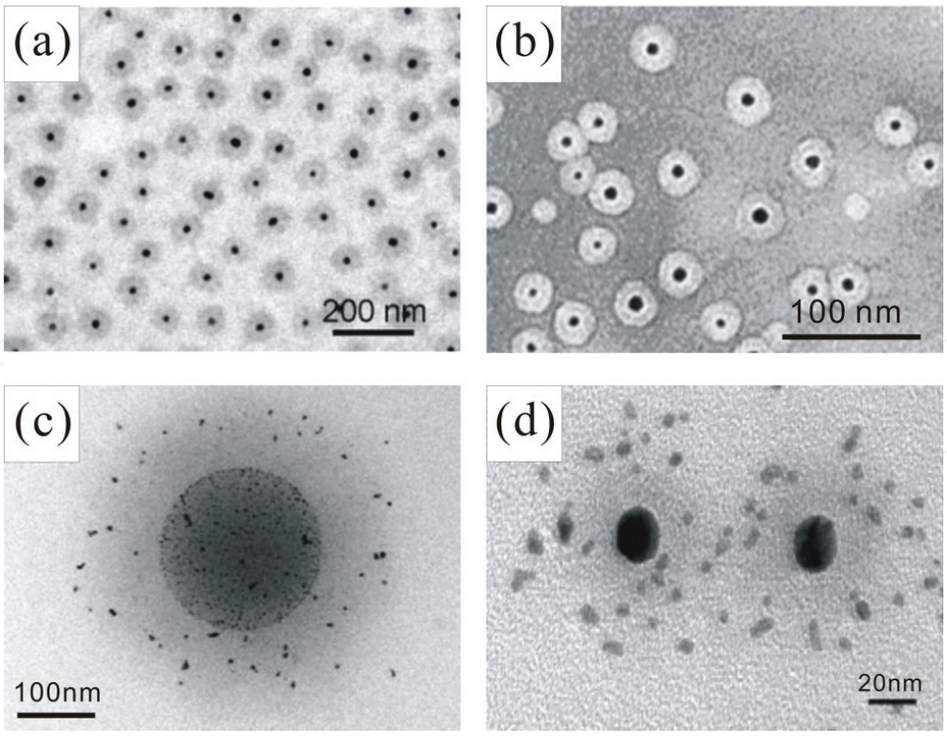

Figure 1. TEM images of metal nanoparticles (dark dots) encapsulated within its polymeric templates: (a) PNIPAm-*b*-PMOEGMA/Au [Taken from Ref. [1]], (b) PS-*co*-PGA/Au [Taken from Ref. [2]], (c) PS/poly (aminoethylmethacrylate HCl)/gold particles PNIPAm-*co*-GMA/Au [Taken from Ref. [3]], and (d) PNIPAm-*b*-PMOEGMA/ Au with Ag [Taken from Ref. [4]].

http://dx.doi.org/10.5772/intechopen.68388

and later, stabilizing agents (e.g., ligands, polymers, or surfactants). Turkevich et al. [6] and Brust-Schiffrin et al. [7] were able to use this similar approach by synthesizing gold nanoparticles. Their synthetic route involved the reaction of a chloroauric acid with sodium citrate solution at boiling temperature ($HAuCl_4 + Na_3C_6H_5O_7 = Au^0$). Later on, Frens [8] was able to control the size formation of gold nanoparticles by varying the reducing agent to gold-salt ratio during the reduction process. Furthermore, Yonezawa and Kunitake [9] used sodium 3-mercaptopropionate to the prestabilized citrate gold nanoparticles. The Brust-Schiffrin's method involves the reduction of gold-salt solution using a thiol-based organic solvent in a two-phase system. The organic layer is separated, evaporated, and mixed with ethanol to get rid of excess thiol. The crude product is further dissolved in toluene and precipitated in ethanol. A modified Brust-Schiffrin process was carried out by Murray et al. [10] or commonly called as "place exchange" process. This process used various functionalities, such as bromine, cyanide, ferrocenyl, alcohol, formaldehyde, and anthraquinone, in replacement of a simple alkane group. Sulfur ligands such as xanthates [11], disulfides [12], di and trithiols [13], and resorcinarene tetrathiols [14] have also been utilized for gold nanoparticles (AuNPs) syntheses. Biphasic methods of AuNP synthesis can also use similar ligands such as phosphine [15], amine [16], carboxylate [17], isocyanides [18], citrate with acetone [19], and iodine [20]. Structures of these ligands are shown in **Figure 2**.

In general, there are three classifications of approaches to prepare AuNPs: (1) nonchemical methods such as electrochemical [21] and thermal decomposition of a metal-salt solution [22], photochemical [23], sonochemical [24], laser ablation synthesis [25], and microwave-assisted technique [26]; (2) biological sources such as the use of plant extracts and microorganism-assisted formation of metal nanoparticles. Bio-reduction of metal ions involves both intracellular and extracellular precipitations of metal nanoparticles within the microorganism (**Figure 3**) [27]. Biomolecules such as proteins are mainly responsible for the synthesis of gold nanoparticles while enzymes produced in the outer layer membrane of the microorganism are responsible for the reduction of gold ions. The biological pathways for metal nanoparticles synthesis

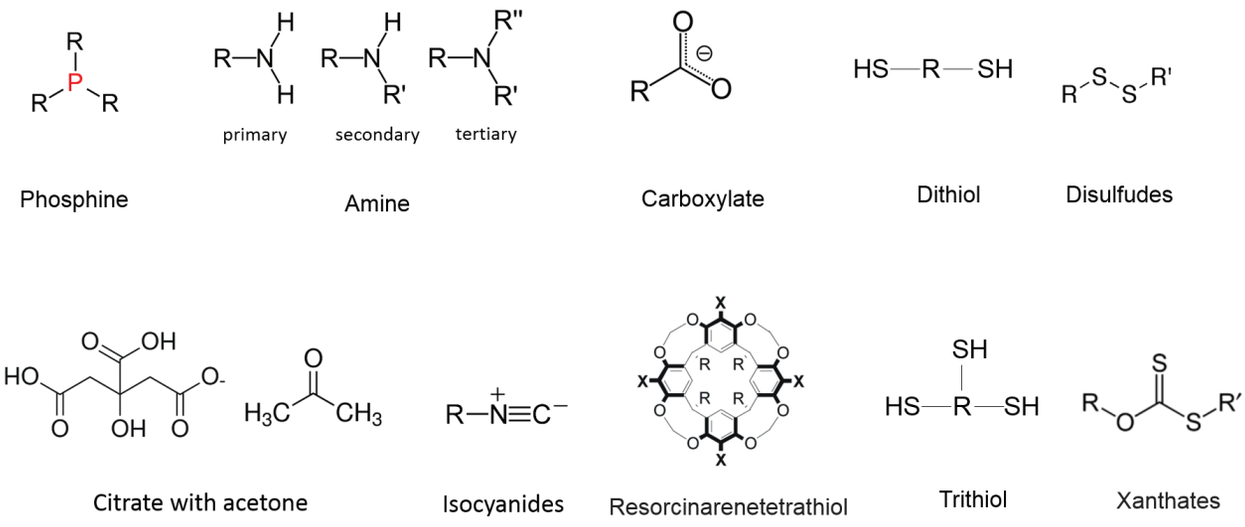

Figure 2. Different ligand molecular structures that can be used for gold nanoparticle synthesis.

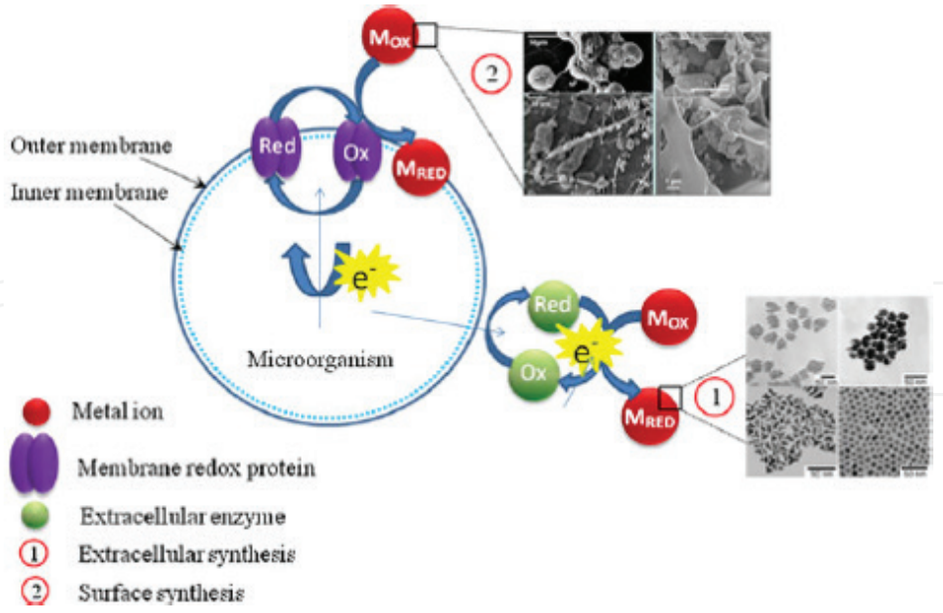

Figure 3. Biosynthetic mechanism of metal nanoparticles using microorganism [Taken from Ref. [27]].

can be carried out by a microorganism (e.g., bacteria [28], yeast (*P. jadini*), and fungal (*V. luteo-album*) cultures [29]), plants [30–32] and plant extracts [33]. In recent years, development of plant extract-based synthesis of metal nanoparticles has been investigated. Using plant-based synthesis results into more stable and faster rate of synthesis compared in the case of microorganism [34]. (3) Use of a polymer as a template for metal nanoparticles (MNPs) generation is commonly called polymer-mediated synthesis. This emerging type of approach was conceived to solve the issue on MNP aggregation.

1.1. Polymer-mediated synthesis of metal nanoparticles

Polymers that have both reducing and stabilizing properties have been developed to synthesize metal nanoparticles. Such dual properties give pure and homogenous products. The main feature of this approach lies on its low cost, high efficiency, and environmentally benign nature. Several existing polymers, which display these dual properties (e.g., reducing and stabilizing metal nanoparticles), have already been used in the synthesis of MNPs such as poly(N-vinyl-2-pyrrolidone) (PVP) [35], poly(allylamine) (PAAm) [36], poly(o-phenylenediamine) (PoPD) [37], polyethyleneimine (PEI) [38], and poly(4-styrenesulfonic acid-co-maleic acid) (PSSMA) [39]. Mechanisms have been studied in the reducing capacity of the PVP. These include a free radical mechanism, oxidation of the hydroxyl end groups [40] and the C=O double bond [41]. Other factors include an abundance of amino groups in the PAAm and PEI molecules that drive the reduction of gold ions into metal nanoparticles and strong bonding between the electrons donor, π orbitals donor, and the lone pair orbitals of amine groups of PoPD with the electron-deficient orbitals of gold nanoclusters providing efficient stabilizing effect. Due to the high impact polymer-assisted approach on the synthesis of metal nanoparticles, several studies came up with some concluded advantages.

http://dx.doi.org/10.5772/intechopen.68388

(1) Only a small concentration of polymer is used. (2) The functional groups in the polymer can serve for dual properties. (3) Polymer template itself can control the size and morphology of MNPs and its resultant composite.

1.2. Core-shell particles (CSP)

With the promising potential of the polymer-assisted approach on the synthesis of metal nanoparticles, the authors make use of polymeric particles. Here, it is referred as core-shell particles (CSP). Some of the commonly used polymers as templates and nanoreactors for metal nanoparticle formation are poly(glycidyl methacrylate-co-N-isopropylacrylamide) [(poly(GMA-co-NIPAM))] [42], poly(N-isopropylacrylamide)-co-poly(acrylic acid) (PNIPAM-co-PAA) [43], glycidyl methacrylate (GMA) and *N*- isopropyl acrylamide (NIPAM) [44], polystyrene (PS) core and a polyaniline (PANI) [45], (poly(N-isopropylacrylamide-acrylic acid) P(NIPAM-AA) [46], long cationic polyelectrolyte chains of poly(2-aminoethyl methacrylate hydrochloride) (PAEMH)) [47], and poly(ionic liquid) (PIL) [48].

Over the past decade, a metal-salt reduction process is the most common method for generating metal nanoparticles. This type of reaction has shown reliability and uniformity of metal nanoparticles produced. However, environmental concerns are not well addressed or worst not met. For example, the use of different forms of energy (e.g., photoirradiation, ultrasound irradiation, and high temperature boiling process) in both electrochemical and thermal decomposition methods is far way exploited [49] in addition to long and tedious synthetic procedures. And worst, giving low yields [50] with a high polydispersity of metal nanoparticles. Such high polydispersity is mostly observed in a reverse microemulsion of metal nanocomposite [51]. For metal nanoparticles bound ligands, the consequence of the difficulty in dispersing in water hinders the surface modification and functionalization for further applications [7]. As a result of this water incompatibility, metal nanoparticle properties are altered [52]. Also, some reducing agents such as sodium borohydride and hydrazine are considered toxic chemicals and not tolerable for future commercial scale-up [53]. Else, defective products or impurities may arise from excess reducing agents [54]. As a result, impurities left behind may eventually affect the composite material's functionality and its potential applications.

With the existing and emerging technologies in the synthesis of metal/polymeric nanocomposites, there is still a great challenge to the concept of Green Chemistry. This concept aims at the development of methods for the synthesis of metal/polymeric in this case, with the least impact on humans and environment as a whole. The challenges in creating novel metal/polymer nanocomposites are: (1) to create a unique template that is an all-in-one platform that can reduce metal ions to nanoparticles, immobilize the resultant nanoparticles, and stabilize the composite particle; (2) to regulate the accessibility of the metal nanoparticles through controlling external stimuli such as pH, temperature, and electrolyte; (3) to immobilize other organic and biological molecules for protection and deliveries; (4) to easily be purified and recovered; (5) to efficiently scale up process for commercialization.

2. Core-shell microgel template and metal/polymeric nanocomposite synthesis

A novel approach was developed with a simple yet versatile synthesis of a variety of amphiphilic core-shell particles [55]. This approach enables to synthesize a broad range of core-shell particles with different chemical structure, composition, size, and functionality. The process uses aqueous-based Chemistry, which is environmentally benign, and the particles are easy to synthesize in high solids content (up to 30%) in the absence of surfactant. A novel feature of this synthetic approach is that it combines graft copolymerization, *in situ* self-assembly of the resulting amphiphilic graft copolymers and emulsion polymerization in a one-step synthesis. In this chapter, core-shell microgels were used in the synthesis of mono (Au) and bimetallic (Au@Ag) nanoparticles. Briefly, the mechanism involved in the core-shell microgel synthesis combines graft copolymerization of vinyl monomer from a water-soluble polymer containing an amino group and self-assembly of the resulting particle. Graft polymerization of vinyl monomer in water happens when amino radicals are formed. The electron transfer and loss of proton form amino radicals during the interaction of alkyl hydroperoxide (ROOH) with the amino group of the polymer backbone (i.e., PEI is mostly used). Alkoxyl radicals (RO) are inevitably produced during this interaction. The resulting amphiphilic macroradicals undergo self-assembly forming micelle-like microdomains, where they become loci for the further polymerization of the monomers. The generated RO·radical on the other hand initiates homopolymerization of the vinyl monomer or creates radicals for further graft polymerization. This process results in well-defined core-shell particle structure with a hydrophilic shell and a hydrophobic core.

2.1. Synthesis of AuNPs in PNIPAm/PEI microgel template

The preparation of the Au nanocomposite (Au/(PNIPAm/PEI)) particles was carried out based on a previous method [56] developed by Tan et al., performed via the addition of hydrogen tetrachloroaurate(III) trihydrate ($HAuCl_4 \cdot 3H_2O$) solution into the as-prepared PNIPAm/PEI. The mixture was continuously stirred and carried out at different temperatures and pHs for 2 hours and heated at 60°C for about an hour. The resulting gold loaded microgels were then purified by centrifugation.

Gold nanoparticle formation in a microgel template is shown in a schematic diagram (**Figure 4**). Such formation from its ionic form is considered to be thermodynamically stable, which does not need any activation energy to form gold nanoparticles even at room temperature. Two successive reactions occur to complete the gold generation. First is the interaction between the negatively charged gold chloride ions ($AuCl_4^-$) and the cationic microgels. Once the gold ions are attracted into the microgel, a subsequent redox reaction occurs between the gold ions and available amine groups in the microgel template. As a result, gold ions are reduced while the amine groups are oxidized. Amine oxidation allows transfer of electrons from the amine to the gold ions, thus, generating zero-state AuNPs. Such reaction was reported by Lala et al. [57], wherein they have proposed that the $AuCl_4^-$ ions are electrostatically bound to

http://dx.doi.org/10.5772/intechopen.68388

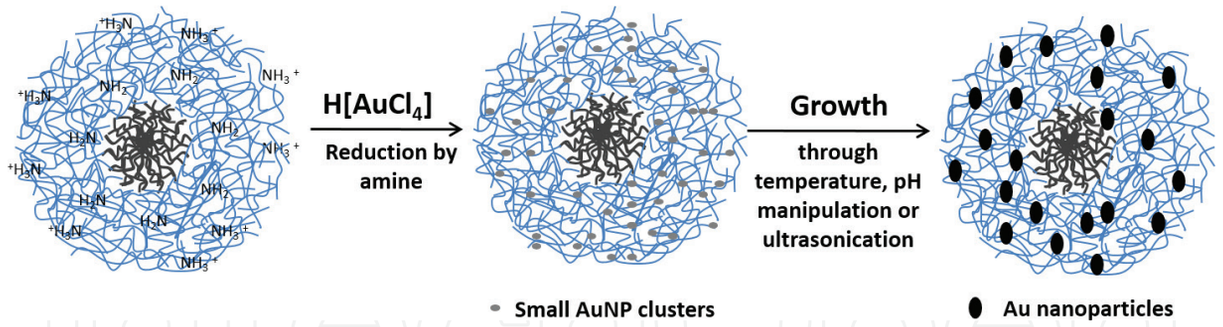

Figure 4. Schematic diagram on the synthesis of gold nanoparticles (AuNPs) using PNIPAm/PEI microgel as a template.

the protonated amine group and simultaneously reduced by the unprotonated amine group. AuNPs clusters were allowed to grow by further heating or manipulating their temperature or pH conditions.

2.2. Synthesis of Au@Ag/core-shell PNIPAm/PEI microgel composite particles

Au@Ag bimetallic nanoparticle synthesis was carried out through a progressive reduction of Au and Ag metal ions as performed previously by Tan et al. [58]. Gold metal ions were first reduced to the shell component of the microgel. These gold metal nanoparticles were then used as a seed for the successive reduction of the silver ions to silver nanoparticles. Appropriate molar ratios of Au^{3+} and Ag^{1+} ions were used and mixed for 30 minutes to reduce the silver ions to metal nanoparticles further, followed by heating at 60˚C for 30 minutes.

Generating bimetallic nanoparticles in a microgel template is shown in a schematic diagram (**Figure 5a**). After the synthesis of microgel template through graft copolymerization, gold clusters were first generated on the shell layers of the templates. Such generation is possible due to hyperbranched PEI in the shell region, which contains amine groups that are known to have reducing ability to generate metal nanoparticles [59]. And through the chelating properties of the same amino groups, PEI can also complex with metal ions and metal nanoparticles [60]. The preformed gold nanoparticles acted as seeds or nucleation sites for further bimetallic nanocrystals formation. Such formation of Au seeds occurred after 30–40 minutes of reaction at room temperature which was evident by the change of the solution color from turbid white to light pink. The transition of the solution color also signifies the change in ionization potential and electron affinity values of Au atoms. Au atoms' ionization potential becomes higher than those of Ag atoms. Such shift results to a larger electronegativity value for Au, wherein significant charge transfer may occur from silver to gold atoms [61]. Simultaneously, silver metal ions (Ag+) were reduced to silver nanoparticles through under-potential deposition mechanism [62], or noble metal induced reduction (NMIR) method [63]. Further, illustration of this mechanism is displayed in **Figure 5b**. It is shown that gold nanoparticles used as a seed for further reduction of silver ions to silver nanoparticles. The AuNP with a bigger size attracts the silver ions resulting to a bimetallic alloy nanoparticle. Further heating was necessary to improve the crystallinity of the bimetallic nanoparticles. Consequently, heating of these composite particles removes partially the template resulting in the naked exposure bimetallic nanoparticles.

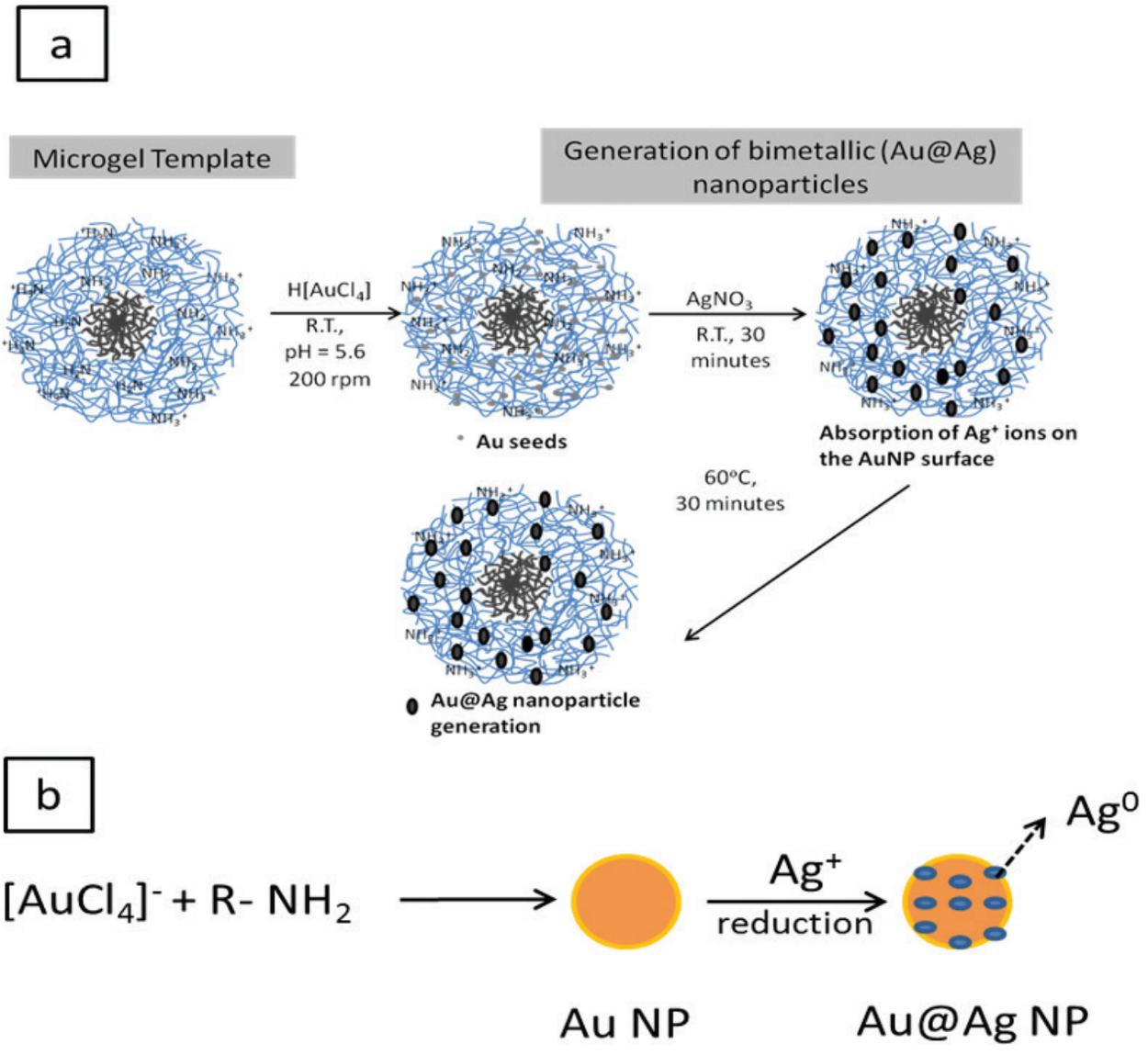

Figure 5. (a) Schematic diagram on the synthesis of bimetallic nanoparticles from Au/PNIPAm/PEI composite particles, (b) mechanism on the formation of Au@Ag nanoparticles from Au/PNIPAm/PEI nanocomposites.

3. Multifunctional roles of PNIPAm/PEI microgel

3.1. Microgel as a nanoreactor

Transmission electron microscope (TEM) images of both the empty PNIPAm/PEI microgel template and the gold nanoparticle-filled composite particles are shown in **Figure 4**. Herein, the empty PNIPAm/PEI microgel particles show a core-shell structure (**Figure 6a**), while AuNP-filled microgel template (**Figure 6b**) shows darks spots around its perimeter. The gold nanoparticles within the microgel template look like clusters of small gold nanoparticles. When heated to 60°C for an hour, the gold nanoparticles further crystallized and became clearer. The size of the gold nanoparticles was roughly estimated at an average of 17.60 ± 2.34 nm with a narrow size distribution.

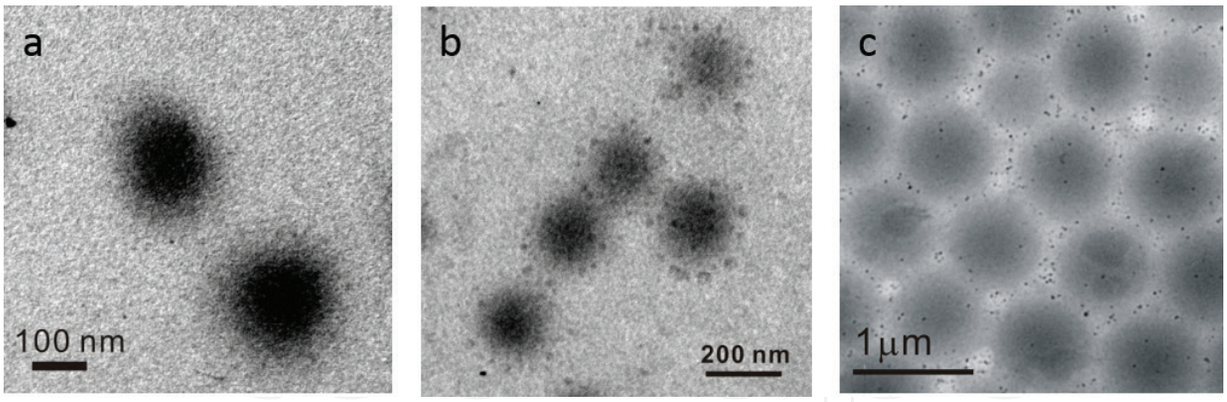

Figure 6. TEM images of the (a) PNIPAm/PEI microgel template, (b) Au/(PNIPAm/PEI) composite particles synthesized at 25°C and pH 7.30, and (c) heated Au/PNIPAm/PEI composite particles.

The kinetics of the formation of gold nanoparticles was monitored through the UV-vis absorbance at 525 nm wavelength with time. Such adsorption at 525 nm wavelength is one characteristic of AuNPs. In **Figure 7**, the increase of the absorbance was fast in the first 30 minutes of reaction and became slower after that, until the third hour of reaction. The reaction started to cease after 3 hours, and no significant change of absorbance was further observed. This data concludes that both electrostatic interaction and reduction of gold ions to nanoparticles simultaneously occurred at a fast rate. This graph further proves that there is a rapid nucleation during the initial stage of gold-ion reduction, resulting in numerous Au clusters. It was further concluded that the reduction of gold ions to AuNPs using microgel was 625 times faster than the naked hyperbranched PEI (linear curve with hollow points).

3.2. Microgel as a stabilizer of AuNPs in composite particles

There are two kinds of stabilization that holds both the AuNPs and the composite material in suspension. Such stabilization is due to the microgel template's property to provide electrostatic interaction between composite particles and steric effect of the PEI shell.

Electrostatic interaction between the composite particles and the gold nanoparticles within the template is the primary contributor to its stabilization. When Au nanoparticles are formed and immobilized in the particle template, the overall size of the composite particle becomes smaller than the pure template itself. This shrinkage is due to the formation of gold/amine complexes resulting in the contraction of the PEI shell. Such contraction of PEI shell reduces metal nanoparticles leaking from its template or its individual network-cage-like structure. Consequently, continuous leaking of naked AuNPs will form aggregates within the template. On the other hand, the same repulsion force acts between composite particles. Such force prevents them from getting attracted to each other preventing them from forming precipitates eventually.

Steric contribution to the stabilization of the AuNPs comes from the hyperbranched structure of the PEI-shell component in the microgel template. This type of stabilization is known in a lot of amphiphilic graft copolymers [64]. Such property of amphiphilic copolymers is due to the hydrophobic-hydrophilic interaction of the copolymers involved. This interaction is very

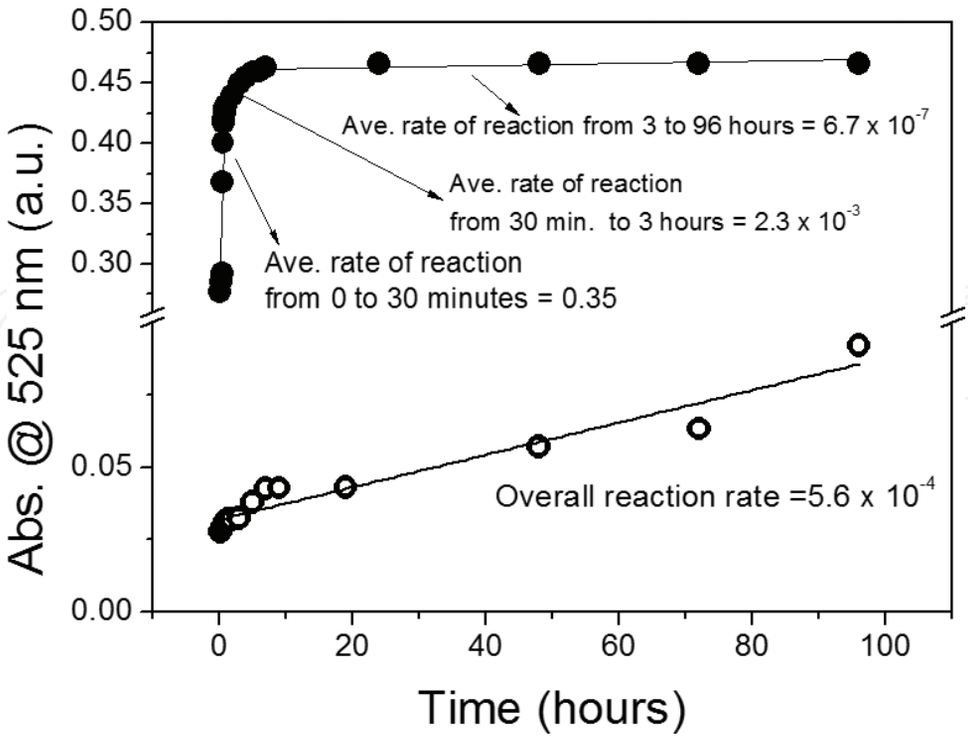

Figure 7. Time courses of the absorbance monitored at 525 nm during the formation of gold nanoparticles in the presence of PNIPAm/PEI microgel particles (25°C, at pH 5.6).

significant on the stability of the microgel template itself and in the formation of Au/microgel composite particles. When this interaction happens in the microgel template, the PEI shell anchors in the gold nanoparticles, while the PNIPAm core is kept together away from the shell. With such action, both the shape and stability of the composite particles are achieved.

3.3. Microgel as AuNP immobilizer

The generated gold nanoparticles using microgel template were immobilized through the template PEI shell's properties. Primarily, the weak bonding between the amino group and the gold nanoparticles is the primary source of immobilization [65, 66]. Such immobilization strongly supported by the hyperbranched nature of the PEI [67], which helps to shield AuNPs into a network-cage like structure. Such construction provides bulkiness and prevents the AuNPs from aggregating with neighboring AuNPs or composite particles. Furthermore, PEI-shell structure can also link the gold nanoparticles intact [68] within its boundary template.

There are five pieces of evidence to demonstrate the microgel acting as an immobilizer of gold nanoparticles: (1) In **Figure 6b**, AuNPs are seen as fuzzy gray dots embedded within the circumference of the microgel, attached in the shell region. (2) There was a decrease in the size of the pure microgel template when loaded with AuNPs. The decrease in size was due to the encapsulation of the gold metal ions attracted to the template. Absorption of the gold metal ions leads to the shrinking of the composite material. (3) There was a decrease in the zeta-potential from 30 to 15 mV from a pure microgel to Au-loaded template, respectively. Such decrease of the zeta-potential is attributed to the partial consumption of the cationic

ammonium ions during the gold-ion adsorption stage. (4) X-ray photoelectron spectroscopy (XPS) (**Figure 14**) result further shows proof of the immobilization of AuNP in microgel template. This result verifies the location of AuNPs which are found within 2—10 nm deep from the surface of the microgel template. (5) The ligand role of the PEI shell (i.e., complexation of the water-soluble PEI with metal ions) plays a significant part of the immobilization of AuNPs. This ligand role property results in some advantages of the composite material such as water solubility, high capacity for metal uptake, easy separation of polymer complexes, high flexibility of the molecular conformation, and good chemical and physical stability [69–71].

3.4. Microgel as a smart controller of AuNP accessibility

One of the best features of PNIPAm/PEI microgel template is its ability to regulate its size. Such ability is useful in the accessibility of the gold nanoparticles generated within the microgel template. This ability of the microgel comes from the stimuli-responsive nature of the PNIPAm or some refer them to smart materials. In the case of PNIPAm/PEI microgel, such sensitivity is based on both sensitive pH and temperature. The core part of the microgel, PNIPAm is temperature sensitive, while the PEI shell is pH sensitive. The response of this soft template to temperature or pH affects its conformational structure. The changes in the structure of the template result in the controlled accessibility of AuNPs as demonstrated in **Figure 8**. Herein, the microgel template loaded with AuNPs is in different sizes under different pH or temperatures. At low pH, the template gets protonated and swells. Such swelling exposes the encapsulated AuNPs. However, when pH increases, the microgel becomes deprotonated and deswelling of the template occurs. By this action of the microgel template, AuNPs embedded within are trapped. The same action also controls that degree of plasmon coupling of AuNPs. Such coupling property originates from the dipole interaction among gold nanoparticles, which allows the control of the interparticle distance between gold nanoparticles [72].

On the other hand, when the temperature of the microgel system reaches beyond the lower critical solution temperature (LCST) point of the core part, PNIPAm (i.e., 32°C), the entire template shrinks. Such shrinking leads to the trapping of AuNPs within the template. But when the temperature goes below the LCST of PNIPAm, the template is more open and loose than the original condition. This looseness results in easy accessibility of the AuNPs within the template.

Microgel particles were subjected to different temperature conditions at 29°C, 45°C, and back to 29°C in aqueous solution to demonstrate the smart properties of the template. Their corresponding structural changes of the microgel particles under different temperatures were captured with AFM analysis. Original microgel template at 29°C in a fluid mode is shown in **Figure 8a** with sizes ranging from 100 to 150 nm with quasi-spherical morphologies. When the temperature was raised to 45°C (**Figure 8b**), the templates decreased in size showing porous surfaces. Such phenomenon is attributed to the shrinking of the templates as it goes beyond its volume phase transition temperature (VPTT). However, when restored to 29°C (**Figure 8c**), the smooth morphology and size of the templates were restored. Such restoration demonstrates that the conformational changes of the template triggered by the response to temperature are reversible.

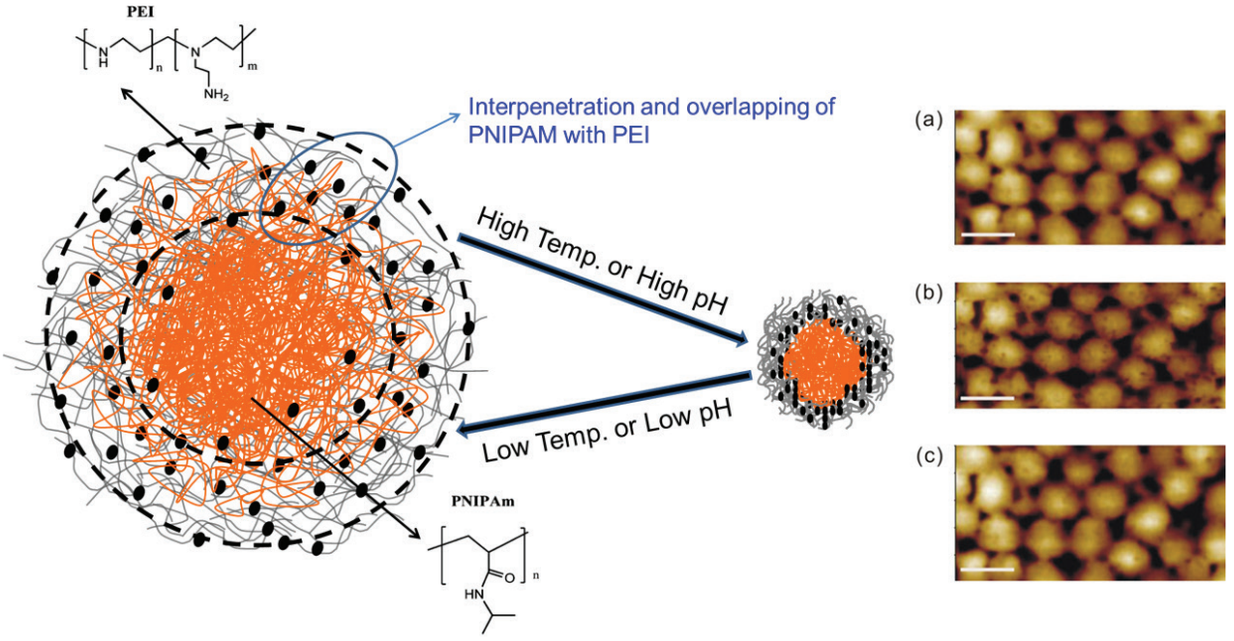

Figure 8. Left side: conformational changes of microgel template from stimuli response to pH solution and temperature. Right side: AFM micrographs of PNIPAM/PEI microgel particles measured in a fluid mode at different temperatures: (a) 29°C; (b) 45°C; and (c) Cooled from 45 to 29°C. Scale bar: 200 nm.

4. Measurements and characterization

4.1. Particle size and surface charge

Dynamic Light spectrophotometer measured the sizes of both pure and gold-loaded microgels. Synthesized PNIPAm/PEI microgels have an average hydrodynamic diameter of 402 nm while the gold-microgel composite particles were measured at 298 nm as shown in **Figure 9a**. The polydispersity indices on both unloaded and gold-loaded particles were 0.050 and 0.055, respectively. As anticipated, the particle size of the gold-loaded microgel is smaller than the pure microgel. This decline in size is due to the incorporation of the counterions into the microgel template during the metal ion absorption and reduction stages. Furthermore, when AuNPs are formed, the microgel network immobilizes *in-situ* generated AuNPs by capturing them on its network-like structure, providing a steric effect on the metal nanoparticles.

The gold-loaded microgel particles were further characterized based on its surface charge expressed in zeta-potential. Gold-loaded composite particles have an average zeta-potential of 15 mV at pH 7.00 in an aqueous medium. At this state, composite particles were stable with no aggregation or precipitation occurred. However, zeta-potential can be affected by the pH solution in a colloidal system. To demonstrate this effect, **Figure 9b** demonstrates the change of the surface charge as a function of pH. In the same figure, gold-loaded microgels can be grouped into a three-phase behavior regarding zeta-potential versus pH solution. The first phase shows a constant zeta-potential behavior at a pH range of 2–6.5. The second phase is between pH 6.5 and 9.0, which shows a noticeable decrease of zeta-potential. The third

http://dx.doi.org/10.5772/intechopen.68388

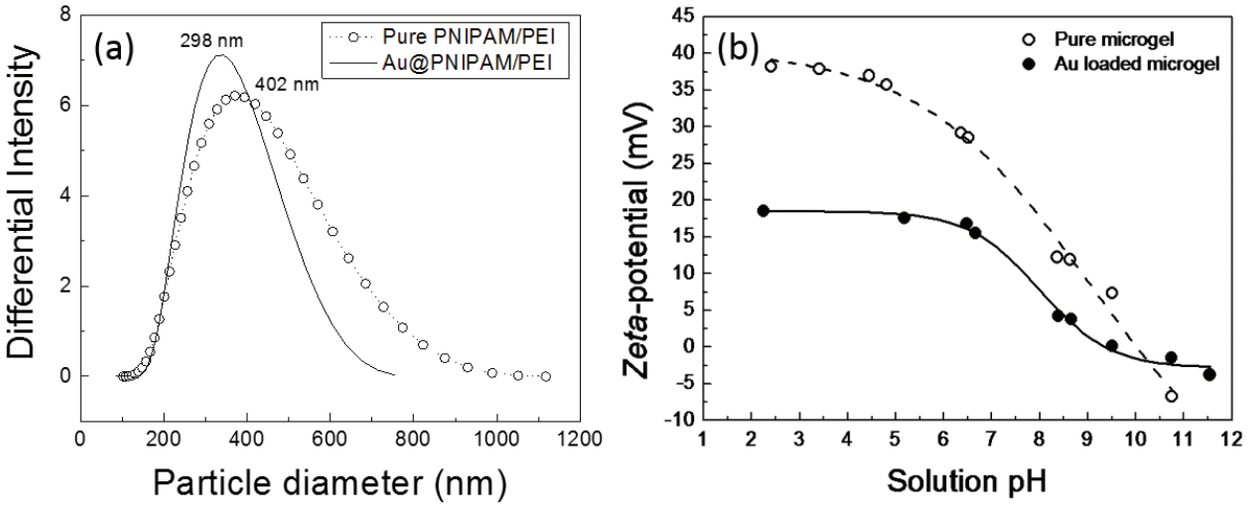

Figure 9. (a) Particle size and size distribution of pure microgel template and Au/(PNIPAm/PEI) composite particles synthesized at optimum conditions of 25°C and pH 7.30. (b) Zeta-potential profile of gold-loaded microgel (solid points) and pure microgel template (hollow points) in different pH solution.

phase between pH 9.0 and 11.5 gives a slight change of zeta-potential values. The constant zeta-potential in the first phase is attributed to the saturation of microgel template with AuNP at this certain range of pH. However, increasing the pH affects the composite material and decreases its surface charge surpassing the isoelectric point (i.e., pH 9.2). Further increase of pH at this stage may supersaturate the microgel template and then again give a very minimal or no effect on its zeta-potential.

To demonstrate the effect of temperature on its surface charge, **Figure 10** shows that varying solution temperatures from 25 to 40°C strongly affect the zeta-potential of both the pure and gold-loaded microgel particles. An abrupt change of surface charge in the temperature range between 29 and 34°C is obvious. This region crosses the VPTT region of the microgels. However, prior and after this temperature range, the zeta-potential was more or less constant. Such behavior is attributed to the increase in the surface charge density of the composite particles with the decrease in size. Smaller particles result in higher surface charge density, resulting in the shrinking of the composite particles, as also observed in the work of Ou et al. [73].

4.2. Scanning electron microscope (SEM) and transmission electron microscope (TEM) images

SEM and TEM images of the AuNP/(PNIPAm/PEI) composite particles are both shown in **Figure 11**. **Figure 11a** shows uniform spherical morphologies of the composite particles. Such morphologies are identical to that of the original microgel template (**Figure 11a** inset). However, partial agglomeration of the particles is also observed which may have occurred during the drying of the SEM sample treatment. **Figure 11b** shows the TEM image of the gold-loaded microgel which shows clearly the location of the AuNPs within the microgel template. Specifically, AuNPs reside around the circumference of the microgel attached in the shell region. Apparently, these images also show the effectiveness of the immobilization of the gold nanoparticles within the microgel network.

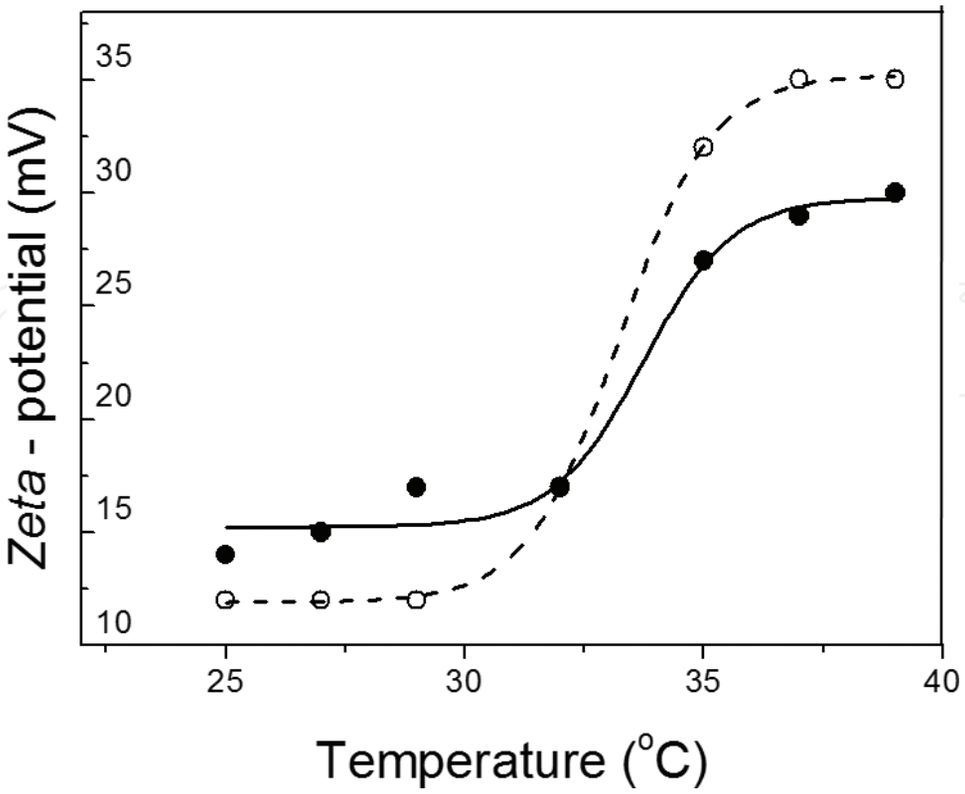

Figure 10. Zeta-potential profile of gold-loaded microgel composite particles (solid points) and pure microgel template (hollow points) in different temperature conditions.

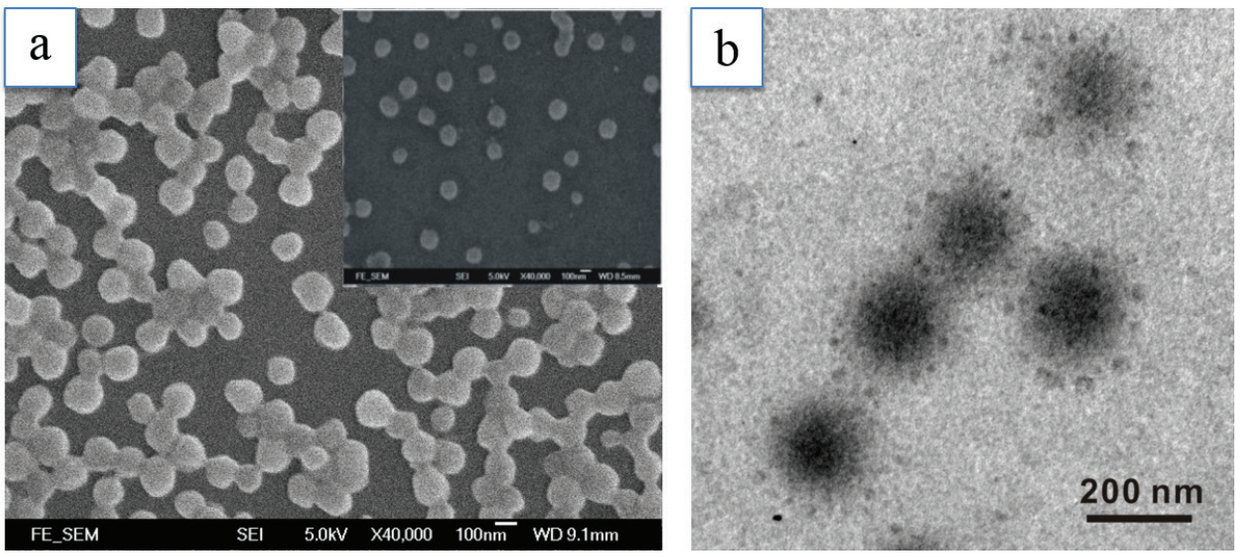

Figure 11. (a) SEM image of Au/ (PNIPAm/PEI) composite particles, inset is the original microgel template, (b) TEM image of Au/ (PNIPAm/PEI) composite particles. The particles were synthesized at 25°C and pH 7.30.

4.3. UV-vis spectroscopy

The formation of gold nanoparticles in the presence of microgel template was monitored by a UV-vis spectroscopy as a function of time. In this case, gold nanoparticle formation was evident at the absorbance wavelength of 525 nm as shown in **Figure 12**. Gold formation starts

http://dx.doi.org/10.5772/intechopen.68388

after 20 minutes of reaction together with the change in color from turbid white to light pink. An increase of absorbance happens as further reaction occurs for gold nanoparticle formation. This also gives rise on the concentration of gold nanoparticle at higher absorbance. After 4 hours of reaction, it was observed that there were no more significant changes in the absorbance intensity, which signify that gold nanoparticles have ceased to grow or gold ions have ultimately been reduced to nanoparticles. Wavelength absorbance of gold nanoparticles ranging from 520 to 525 nm is a characteristic of Au nanoparticles with spherical shape with sizes ranging from 15 to 30 nm [74].

4.4. High-resolution TEM (HRTEM) and X-ray diffraction

To get a closer look at the image of AuNPs immobilized within the PNIPAm/PEI microgels template, an HRTEM analysis was performed as shown in **Figure 13a**. This image reveals a five-fold twinned Au nanocrystal with a diameter of 22.5 nm. Top inset of **Figure 13a** displays the selected-area of electron diffraction (SAED) pattern of AuNPs examined, which reveals ring patterns indexed as (111), (200), and (222) of a face-centered cubic (FCC) gold lattice. Furthermore, this five-fold twinned boundary at the center of an Au nanocrystal can suggest formation of a multiply twinned particle (MTP) close to an icosahedral gold nanostructure. The fuzzy portion observed on TEM image is attributed to the composite particle's sensitivity to misorientation and distortion of the ideal icosahedrons. Aside from the twin boundary observed, the Au nanostructure is mainly composed of (111) planes with a d-spacing of 0.236 nm as shown in **Figure 13b**. The lattice plane is separated by a twin boundary indicated as a white line on the image. The crystallinity of AuNPs embedded in the microgel template is

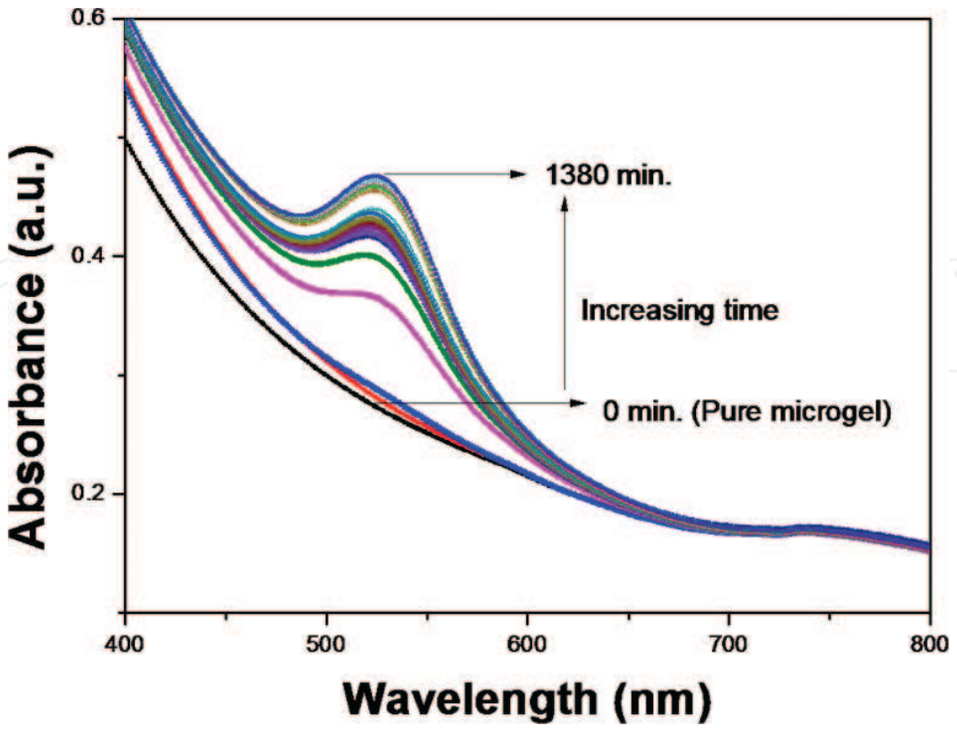

Figure 12. UV-vis spectra profile for reduction of gold ions to nanoparticles using a PNIPAm/PEI microgels versus time (minute). Experiment was performed at 25°C, pH 5.6, 200 rpm, with N/Au molar ratio of 28.5.

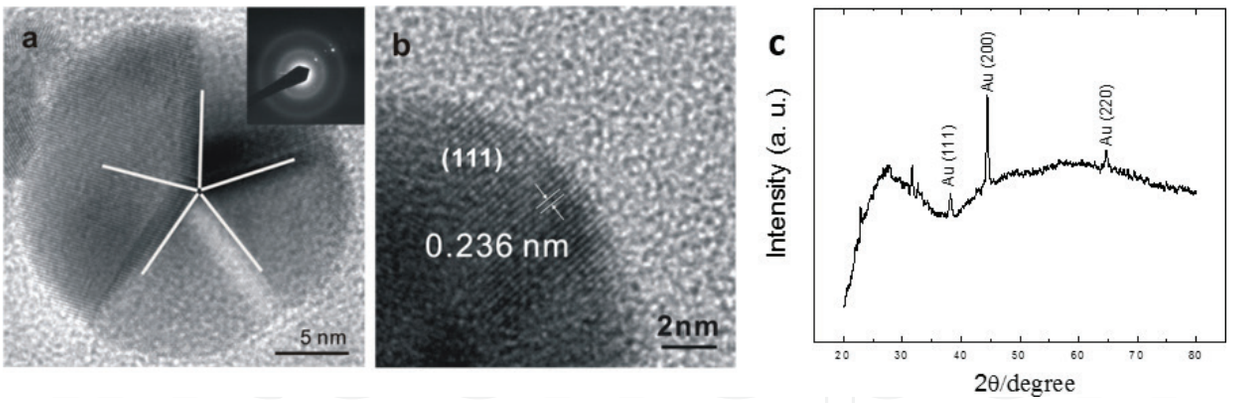

Figure 13. (a) HRTEM image of Au nanoparticle embedded within a microgel template, inset is the selected-area electron diffraction (SAED) pattern, (b) (111) planes of Au nanocrystal with a *d*-spacing of 0.236 nm, and (c) XRD spectra of Au/PNIPAm/PEI composite particles.

analyzed through an X-ray diffractometer in **Figure 13c**. Au nanocrystals formed have lattice arrangements of (111), (200), and (220) at corresponding angles of 38, 44, and 65o. This result is consistent with the previous SAED analysis except for the (220) lattice with a dominant (111) arrangement.

4.5. Surface composition using X-ray photoelectron spectroscopy

To further investigate the formation of AuNPs using a microgel template, X-ray photoelectron spectroscopy (XPS) analysis at a depth of 10 nm was used. Results shown in **Figure 14** reveal an XPS spectra with binding energies of different elements present in the composite particles. The binding energies correspond to elements of C, O, N, and Au. Convoluted C1s spectra were fitted with peaks at 285.0 and 287.9 eV, assigned to C-C/C-H and C-O bonds, respectively. N1s peak fitted at 399.3 assigned to amines coordinated with AuNPs. O1s at 531.2 eV corresponds to the carbonyl functional group of the microgel. Zero-valent AuNPs are observed from its two peak characteristics at 84.3 and 88 eV, consistent with literature [75]. Other characteristic of AuNP is its XPS spectra peak-to-peak distance of 3.7 eV on the Au 4f doublet which further gives a standard measure of the Au^0 oxidation state [76]. As the AuNPs attached to the amino groups, detection of N1s in the XPS analysis weakens due to the overlapping of AuNPs on the amine group [77], eventually strengthening the Au signal. This amine-gold interaction was also observed in the work of Kumar et al. [78] and similar to Manna et al. [79]. Nitrogen peak was also curve fitted into two components at 399.3 and 401.2 eV. The first one corresponds to the amine (free and coordinated to gold) and the other corresponds to the protonated amine or ammonium. With the presence of these two peaks, AuNP binding to the amine group is more on metal-ligand coordination (metallic gold atom and amine) than electrostatic interaction (between ammonium and the negative charges on the surface of the particles).

Further study on the same XPS spectra indicates that there was no significant change of O1s to C1s ratio before and after gold loading. Such insignificant change further proves the presence of the carbonyl functional group, PNIPAm, in the microgel. The XPS spectra also mean that at a depth of at most 10 nm, PNIPAm is present within the shell region partially overlapping the

http://dx.doi.org/10.5772/intechopen.68388

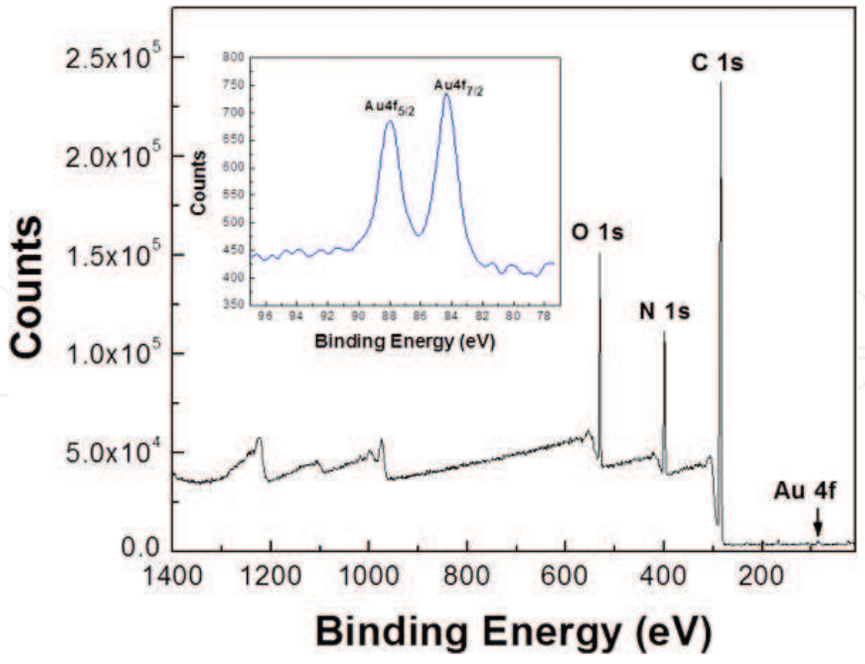

Figure 14. XPS spectra of AuNP embedded in PNIPAm/PEI microgel template. Inset is the Au 4f core-level spectra.

core. With this overlapping of shell component to the core makes the whole microgel system shrink whenever PNIPAm shell becomes sensitive to temperature. Such phenomenon further verifies our claim that the amine group residing in the PEI shell l is mainly responsible for the formation and binding of the AuNPs.

5. Catalytic activities of gold/microgel and gold@silver/microgel nanocomposite particles

To demonstrate the catalytic activity of gold and gold@silver nanoparticles in a microgel template, a catalytic reduction first order kinetic model (i.e., *p*-nitrophenol reduction by sodium borohydride) was chosen. Silver and gold metal nanoparticles have a wide absorption band in the visible region of the electromagnetic spectrum. Thus, they are easy to characterize and with a wide availability of related literature. These metal nanoparticles have also been involved in many catalytic organic reactions and synthesis in both pure and alloyed form. Previous study suggests that silver preserves the overall spherical morphology of the resultant bimetallic eventually prevents the tendency to phase segregate [85]. These are the primary reasons why these two metals have been chosen to demonstrate the metal nanoparticle forming capabilities of the microgel (i.e., PNIPAm/PEI) template. The *p*-nitrophenol solution exhibits a typical absorption peak at around 320 nm under neutral or acidic condition. When sufficient amount of $NaBH_4$ is added, the nitrophenolate ions become the dominant species and reduce to aminophenol. Such conversion causes the absorption peak to shift to 400 nm. In the absence of any catalyst, the reduction of *p*-nitrophenol by $NaBH_4$

cannot proceed based on a control experiment. And theoretically, this is because the E_o value for the reduction of *p*-nitrophenol to *p*-aminophenol was −0.76 V and that of H_3BO_3/BH_4^- was −1.33 V versus the standard hydrogen electrode (NHE). However, when a reduction of *p*-nitrophenol starts, a new peak appears at about 310 nm, which corresponded to the typical absorption peak of *p*-aminophenol Physical change on the solution color is also obvious during the reaction [80]. For the case of gold@silver metal nanoparticle as catalyst, it only took 2 minutes to complete the catalytic reaction (**Figure 15a**). When using monometallic Au catalyst, catalytic reactions were completed in 15 minutes and 3.5 minutes using different amine to gold ratios (i.e., 28.2 and 14.09, respectively). The catalytic activity of the bimetallic catalyst is obviously higher than that of the monometallic catalyst using the same template.

The kinetic rate constant, which is proportional to its overall kinetic rate in a first order reaction, was estimated from its slope. The control sample has a rate constant of 5.4×10^{-3} s^{-1}. However, when monometallic gold nanoparticles (N/Au = 28.20 mole ratio) was used as a catalyst, the reaction proceeded approximately 10 times faster (i.e., with a rate constant of 2.44×10^{-2} s^{-1}) than without catalysts. Moreover, when bimetallic gold@silver nanoparticles were used as a catalyst, the reaction rate was significantly enhanced. The enhancement in catalytic activity is attributed to the synergistic effects and the flexible design between the two metal nanoparticles [81], in this case gold and silver nanoparticles. The electronic and geometrical properties of the synthesized bimetallic nanoparticles can also affect the catalytic activity. Similar studies suggest that the increase in the number of low coordination number, edge and corner sites can also enhance catalytic activity [82]. Surface science studies conclude that the surface electronic structure can be modified by the interactions between the two kinds of atoms in the bimetallic alloy owing to ligand [83] and strain effects [84]. **Figure 15b** shows comparison of the different catalytic reaction rates constants by plotting ln (C_t/C_0) versus

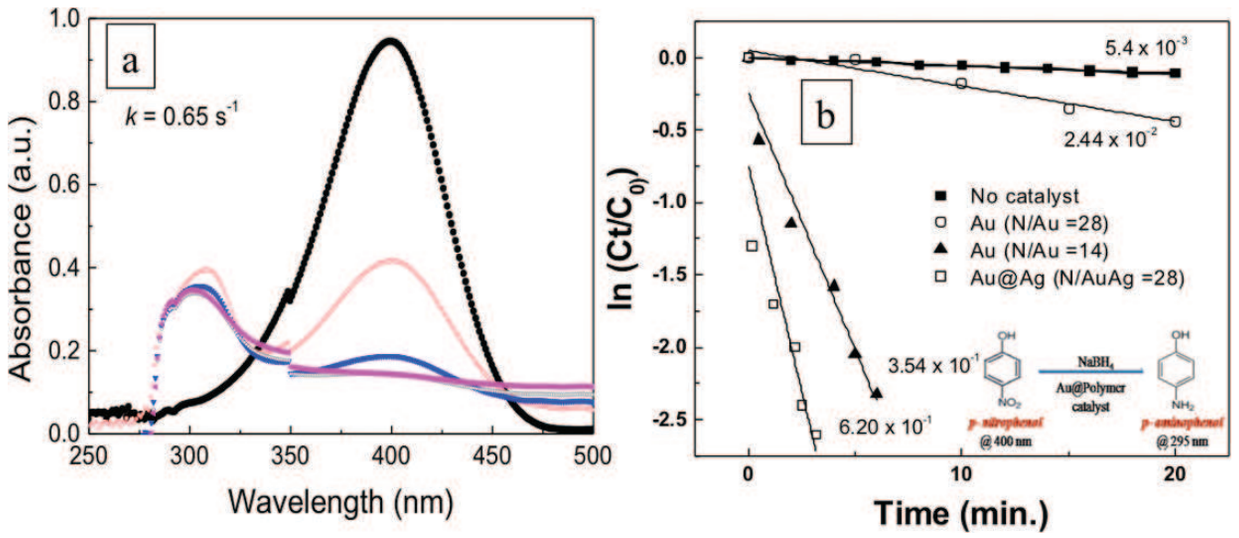

Figure 15. (a) UV-vis spectroscopy profile for the reduction of *p*-nitrophenol to *p*-aminophenol using Au@Ag/(PNIPAm/PEI) composite particle as a catalyst. The different colored-curves refer to the different 30 second time intervals, (b) plot of ln (C_t/C_0) as a function of time for the reaction catalyzed by Au/PNIPAm/PEI in different N/Au mole ratios and Au@Ag bimetallic nanoparticles in PNIPAm/PEI template. Inset is the reaction scheme of the catalytic reaction model used (i.e., reduction of *p*-nitrophenol to *p*-aminophenol).

http://dx.doi.org/10.5772/intechopen.68388

reaction time for the reduction of *p*-nitrophenol. The results demonstrate that the increase or incorporation of different metal nanoparticles can significantly increase the reduction rate.

5.1. Modification of AuNP to Au@Ag bimetallic NP and its effect on catalysis

The main goal in making bimetallic nanoparticles is to enhance the catalytic activity in the reduction of *p*-nitrophenol to *p*-aminophenol. Through the introduction of silver ions into the as-prepared seed gold nanoparticles, surface modification was achieved in the resultant bimetallic Au@Ag nanoparticles. This modification affects the electronic properties of the resultant bimetallic nanoparticles affecting the catalytic activities. Thus, the role of the Ag in the bimetallic structure is a co-catalyst able to promote the ligand effect [85].

Ligand effect suggests that with the presence of a co-catalyst, Ag is important for the redox reaction (i.e., reduction of *p*-nitrophenol) occurring on Ag@Au interfaces [86]. These Ag@Au interfaces are the main actors in improving the catalytic activities. **Figure 16** demonstrates an Ag@Au interface with different work functions (i.e., Au (~5.3 eV) and Ag (~4.7 eV)). Since Ag has a lower work function compared to Au, electrons leave from the Ag atom side of the interface toward the Au side through a depleted region (Region D). As a result, the Au becomes an electron-rich region (Region E). The abundance of electrons on the Au side initiates the uptake of electron from the reactants (i.e., *p*-nitrophenol) on top of the usual uptake from the depleted region. Thus, the more interfaces there are the more depletion and surplus of electron exist, resulting to increase the adsorption of reactants to be reduced on top of the interfacial regions. Such mechanism is consistent with the study of Zhang et al. [87] wherein the increasing electronegativity of Au with

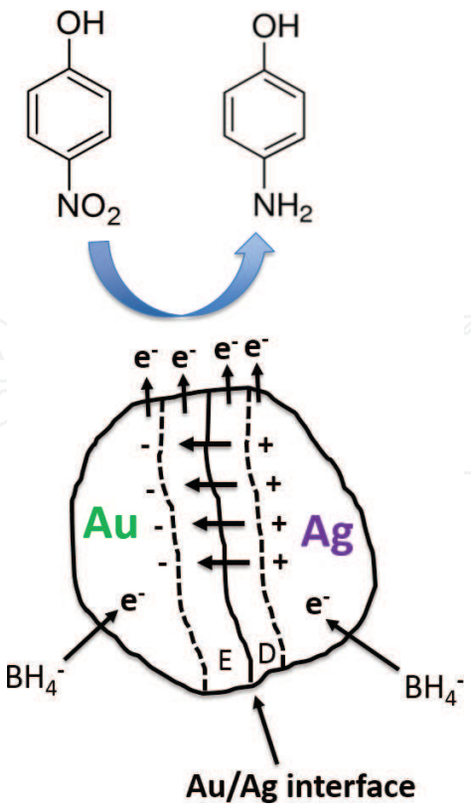

Figure 16. Diagram on the transport of electron from an Ag-Au interface bimetallic NP [Adopted from Ref. [87]].

respect to Ag facilitates adsorbate binding, increasing the electron transfer to *p*-nitrophenol. As a result, this reduces the activation energy barrier, thus increasing the catalytic activity.

6. Conclusion

Environment-friendly approach on the synthesis of metal/polymeric nanocomposite particles was demonstrated in this chapter through the fabrication of Au and Au@Ag nanoparticles using a microgel template (i.e., PNIPAm/PEI). PNIPAm/PEI microgel template plays a crucial role in the reduction of metal salts, stabilization, and immobilization of the resulting metal/polymer nanocomposites. Furthermore, it can also act as a regulator of metal nanoparticles. Catalytic activities of the Au and Au@Ag metal nanoparticles in microgel template were also demonstrated in the reduction of *p*-nitrophenol to *p*-aminophenol.

Acknowledgements

We highly acknowledge the Hong Kong Polytechnic University that has given us the chance to explore our interests in Applied Chemistry. And we are grateful to everyone who inspired us to write this chapter.

Author details

Noel Peter Bengzon Tan[1]* and Cheng Hao Lee[2]

*Address all correspondence to: bengzontan@nami.org.hk

1 Environmental Technologies Section, Nano and Advanced Materials Institute, Ltd., Hong Kong

2 Department of Applied Biology and Chemical Technology, The Hong Kong Polytechnic University, Hong Kong

References

[1] Li D, Cui Y, Wang K, Hem Q, Yan X, Li J. Thermosensitive nanostructures comprising gold nanoparticles grafted with block copolymers. Advanced Functional Materials. 2007;**17**:3134–3140. DOI: 10.1002/adfm.200700427

[2] Li D, He Q, Li J. Smart core/shell nanocomposites: Intelligent polymers modified gold nanoparticles. Advances in Colloid and Interface Science. 2009;**149**:28–38. DOI: 10.1016/j.cis.2008.12.007

[3] Welsch N, Ballauff M, Lu Y. Microgels as nanoreactors: Applications in catalysis. Advances in Polymer Science. 2010;**234**:129. DOI: 10.1007/12_2-10_71

[4] Li D, He Q, Cui Y, Wang K, Zhang X, Li J. Thermosensitive copolymer networks modify gold nanoparticles for nanocomposite entrapment. Chemistry – A European Journal. 2007;**13**:2224–2229. DOI: 10.1002/chem.200600839

[5] Faraday M. The bakerian lecture: Experimental relations of gold (and other metals) to light. Philosophical Transactions of the Royal Society. 1857;**147**:145–181. DOI: 10.1098/rstl.1857.0011

[6] Turkevich J, Stevenson PC, Hillier J. A study on the nucleation and growth processes in the synthesis of colloidal gold. Discussions of the Faraday Society. 1951;**11**:55–75. DOI: 10.1039/DF9511100055

[7] Brust M, Walker M, Bethell D, Schiffrin DJ, WHyman RJ. Synthesis of thiol-derivatised gold nanoparticles in a two-phase liquid-liquid system. Journal of the Chemical Society, Chemical. Communications. 1994;1:801–802. DOI: 10.1039/C39940000801

[8] Frens G. Controlled nucleation for the regulation of the particle size in monodisperse gold suspensions. Nature: Physical Science 1973;**241**:20–22

[9] Yonezawa T, Kunitake T. Practical preparation of anionic mercapto ligand-stabilized gold nanoparticles and their immobilization. Colloids and Surfaces A: Physicochemical and Engineering Aspects. 1999;**149**:193–199. DOI: 10.1016/S0927-7757(98)00309-4

[10] Hoshetler MJ, Templeton AC, Murray RW. Dynamics of place-exchange reactions on monolayer-protected gold cluster molecules. Langmuir. 1999;**15**:3782–3789. DOI: 10.1021/la981598f

[11] Tzhayik O, Sawant P, Efrima S, Kovalev E, Klug JT. Xanthate capping of silver, copper, and gold colloids. Langmuir. 2002;**18**:3364–3369. DOI: 10.1021/la015653n

[12] Porter Jr LA, Ji D, Westcott SL, Grape M, Czernuszewicz RS, Halas NJ, Lee TR. Gold and silver nanoparticles functionalized by the adsorption of dialkyl disulfides. Langmuir. 1998;**14**:7378–7386. DOI: 10.1021/la980870i

[13] Resch R, Baur C, Bugacor A, Koel BE, Echternach PM, Madhukar A, Montoya N, Requicha AAG, Will P. Linking and manipulation of gold multinanoparticle structures using dithiols and scanning force microscopy. Journal of Physical Chemistry B. 1999;**103**:3647–3650. DOI: 10.1021/jp984508o

[14] Balasubramanian R, Kim B, Tripp SL, Wang X, Lieberman M, Wei A. Dispersion and stability studies of resorcinarene-encapsulate gold nanoparticles. Langmuir. 2002;**18**:3676–3681. DOI: 10.1021/1a0156107

[15] Weare WW, Reed SM, Warner MG, Hutchison JE. Improved synthesis of samll (dcore = 1.5 nm) phosphine-stabilized gold nanoparticles. Journal of the American Chemical Society. 2000;**122**:12890–12891. DOI: 10.1021/ja002673n

[16] Heath JR, Brandth L, Leff DV. Synthesis and characterization of hydrophobic, organically-soluble gold nanocrystals functionalized with primary amines. Langmuir. 1996;**12**:4723–4730

[17] Selvakannan PR, Mandal S, Phadtane S, Pasricha R, Sastry M. Capping of gold nanoparticles by the amino acid lysine renders them water-dispersible. Langmuir. 2003;**19**: 3545–3549. DOI: 10.1021/la026906v

[18] Joo SW, Kim WJ, Yoon WS, Choi IS. Adsorption of 4,4'-biphenyl diisocyanide on gold nanoparticle surface investigated by surface-enhanced raman scattering. Journal of Raman Spectroscopy. 2003;**34**:271–275. DOI: 10.1002/jrs.994

[19] Li G, Lauer M, Schulz A, Boettcher C, Li F, Fuhrhop JH. Spherical and planar gold(0) nanoparticles with a rogod gold(I)-anion or a fluid gold(0)-acetone surface. Langmuir. 2003;**19**:6483–6491. DOI: 10.1021/ia0300277

[20] Cheng W, Dong S, Wang E. Iodine-induced gold nanoparticle fusion/fragmentation/aggregation and iodine-linked nanostructured assemblies on a glass substrate. Angewandte Chemie International Edition. 2003;**42**:449–452. DOI: 10.1002/anie.200390136

[21] Reetz MT, Helbig, W. Size-selective synthesis of nanostructured transition metal clusters. Journal of the American Chemical Society B. 1994;**116**:7401–7402. DOI: 10.1021/ja00095a051

[22] Bakrania SD, Rathore GK, Wooldrige MS. An investigation of the thermal decomposition of gold acetate. Journal of Thermal Analysis and Calorimetry. 2009;**95**:117–122. DOI: 10.1007/s10973-00809173-1

[23] Huang WC, Chen YC. Photochemical synthesis of polygonal gold nanoparticles. Journal of Nanoparticle Research. 2008;**10**:697–702. DOI: 10.1007/s11051-007-9293-8

[24] Okitsu K, Mizukoshi Y, Yamamoto TA, Maeda Y, Nagata Y. Sonochemical synthesis of gold nanoparticles on chitosan. Materials Letters. 2007;**61**:3429–3231. DOI: 10.1016/j.matlet.2006.11.090

[25] Amendola V, Polizzi S, Meneghetti M. Laser ablation synthesis of gold nanoparticles in organic solvents. Journal of Physical Chemistry B. 2006;**110**:7232–7237. DOI: 10.1021/jp0605092

[26] Seol SK, Kim D, Jung S, Chang WS, Kim JT. One-step synthesis of PEG-coated gold nanoparticles by rapid microwave heating. Journal of Nanomaterials. 2013;**2013**:531760. DOI: 10.1155/2013/531760

[27] Das SK, Marsili E. A green chemical approach for the synthesis of gold nanoparticles: Characterization and mechanistic aspect. Reviews in Environmental Science and Biotechnology. 2010**;9:**199–204. DOI: 10.1007/s11157-010-9188-5

[28] Lengke MF, Southam G. The effect of thiosulfate-oxidizing bacteria on the stability of the gold-thiosulfate complex. Geochimica et Cosmochimica Acta. 2005;**69**:3759–3772. DOI: 10.1016/j.gca.2005.03.012

[29] Gericke M, Pinches A. Biological synthesis of metal nanoparticles. Hydrometallurgy 2006, **83**, 132–140. DOI:10.1016/j.hydrometl.2006.03.019.

[30] Shukla R, Nune SK, Chanda N, Katti K, Mekapothula S, Kulkarni RR, Welshons WV, Kannan R, Katti K V. Soybeans as a phytochemical reservoir for the production and stabilization of biocompatible gold nanoparticles. Small. 2008;**4**:1425–1436. DOI: 10.1002/smll.200800525

[31] Gardea-Torresdey JL, Parsons JG, Gomez E, Videa P, Troiani HE, Santiago P, Jose-Yacaman M. Formation and growth of Au nanoparticles inside live Alfalfa plants. Nano Letters. 2002;**2**:397–401. DOI: 10.1021/nl015673+

[32] Huang J, Li Q, Sun D, Lu Y, Su Y, Yang X, Wang H, Wang Y, Shao W, He N, Hong J, Chen C. Biosynthesis of silver and gold nanoparticles by novel sundried *Cinnamomum camphora* leaf. Nanotechnology. 2007;**18**:105104. DOI: 10.1088/0957-4484/18/10/105104

[33] Song JY, Jang HK, Kim BS. Biological synthesis of gold nanoparticles using *Magnolia kobus* and *Diopyros kaki* leaf extracts. Process Biochemistry. 2009;**44**:1133–1138. DOI: 10.1016/j.procbio.2009.06.005

[34] Iravani S. Green synthesis of metal nanoparticles using plants. Green Chemistry. 2011;**13**:2638–2650. DOI: 10.1039/C1GC5386B

[35] Chen HJ, Wang YL, Wang YZ, Dong SJ, Wang EK. One-step preparation and characterization of PDDA-protected gold nanoparticles. Polymer. 2006;**47**:763–766. DOI: 10.1016/j.polymer.2005.11.034

[36] Sardar R, Park JW, Shumaker-Parry JS. Polymer-induced synthesis of stable gold and silvernanoparticles and subsequent ligand exchange in water. Langmuir. 2007**;23**: 11883–11889. DOI: 10.1021/la702359g

[37] Han J, Liu Y, Li L, Guo R. Poly (o-phenylenediamine) submicroshpere-supported gold nanocatalyst: Synthesis, characterization, and application in selective oxidation of benzyl alcohol. Langmuir. 2009;**25**:11054–11060. DOI: 10.1021/la901373t

[38] Kuo PL, Chen CC, Jao MW. Effects of polymer micelles of alkylated polyethyleneimines on generation gold nanoparticles. Journal of Physical Chemistry B. 2005;**109**:9445–9450. DOI: 10.1021/jp050136p

[39] Cai LJ, Wang M, Hu Y, Qian DJ, Chen M. Synthesis and mechanistic study of stable water-soluble noble metal nanostructures. Nanotechnology. 2011;**22**:285601. DOI:10.1088/0957-4484/22/28/285601.

[40] Wahio I, Xiong YJ, Yin YD, Xia YN. Reduction by the end groups of poly (vinylpyrrolidone): A new and versatile route to the kinetically controlled synthesis of Ag triangular nanoplates. Advanced Materials. 2006;**18**:1745–1749. DOI: 10.1002/adma.200600675

[41] Huang HH, Ni XP, Loy GL, Chew CH, Tan K L, Loh FC, Deng JF, Xu GQ. Photochemical formation of silver nanoparticle in poly (*N*-vinylpyrrolidone). Langmuir. 1996;**12**:909–912. DOI: 10.1021/la950435d

[42] Suzuki D, Kawaguchim H. Gold nanoparticle localization at the core surface by using thermosensitive core-shell particle as a template. Langmuir. 2005;**21**:12016–12024. DOI: 10.1021/la0516882

[43] Dong Y, Ma Y, Zhai T, Zeng Y, Fu H, Yao J. A novel approach to the construction of core-shell gold-polyaniline nanoparticles. Nanotechnology. 2007;**18**:455603. DOI: 10.1088/0957-4484/18/45/455603

[44] Suzuki D, Kawaguchi H. Hybrid microgels with reversibly changeable multiple brilliant color. Langmuir. 2006;**22**:3818–3822. DOI: 10.1021/la052999f

[45] Liu Y, Feng X, Shen J, Zhu JJ, Hou W. Fabrication of a novel glucose biosensor based on a highly electroactive polystyrene/polyaniline/Au nanocomposite. Journal of Physical Chemistry B. 2008;**112**:9237–9242. DOI: 10.1021/jp801938w

[46] Gorelikov I, Field LM, Kumacheva E. Hybrid microgels photoresponsive in the near-infrared spectral range. Journal of the American Chemical Society. 2004;**126**:15938–15939. DOI: 10.1021/ja0448869

[47] Suzuki D, Kawaguchi H. Modification of gold nanoparticle composite nanostructure using thermosensitive core-shell particle as a template. Langmuir. 2005;**23**:8175–8179. DOI: 10.1021/la0504356

[48] Yuan J, Wunder S, Warmuth F, Lu Y. Spherical polymer brushes with vinlimidazolium-type poly (ionic liquid) chains as supported for metallic nanoparticles. Polymer. 2012;**53**:43–49. DOI: 10.1016/j.polymer.2011.11.031

[49] Alexandridis P. Gold nanoparticle synthesis, morphology control, and stabilization facilitated by functional polymers. Chemical Engineering and Technology. 2011;**34**:15–28. DOI: 10.1002/ceat.201000335

[50] Li W, Jia QX, Wang HL. Facile synthesis of metal nanoparticles using conducting polymer colloids. Polymer. 2006; **47**:23–26. DOI: 10.1016/j.polymer.2005.11.032

[51] Ingert D, Pileni MP. Limitations in producing nanocrystals using reverse micelles as nanoreactors. Advanced Functional Materials. 2001;**11**:136–139. DOI: 10.1002/1616-3028(200104)11:2<136::AID-ADFM136>3.0.CO;2-3

[52] Alvarez MM, Khoury JT, Schaaff TG, Shafigullin MN, Vezmar I, Whetten RL. Optical absorption spectra of nanocrystal gold molecules. Journal of Materials Chemistry B. 1997;**101**:3706–3712. DOI: 10.1021/jp962922n

[53] Nalawade P, Mukherjee T, Kapoor S. Green synthesis of gold nanoparticles using glycerol as a reducing agent. Advances in Nanoparticles. 2013;**2**:78–86. DOI: 10.4236/anp.2013.22014

[54] Meristoudi A, Pispas S. Polymer mediated formation of corona-embedded gold nanoparticles in block polyelectrolyte micelles. Polymer. 2009;**50**:2743–2751. DOI: 10.1016/j.polymer.2009.04.045

[55] Ho KM, Li WY, Wong CH, Li P. Amphiphilic polymeric particles with core-shell nanostructures: emulsion-based syntheses and potential applications. Colloid and Polymer Science. 2010;**288**:1503–1523. DOI: 10.1007/s00396-010-2276-9

[56] Tan NPB, Lee CH, Chen L, Ho KM, Lu Y, Ballauff M, Li P. Facile synthesis of gold/polymer nanocomposite particles using polymeric amine-based particles as dual reductants and templates. Polymer. 2015;**76**:271–279. DOI: 10.1016/j.polymer.2015.09.015

[57] Lala NL, Deivraj TC, Lee JY. Auto-deposition of gold on chemically modified polystyrene beads. Colloids and Surfaces A: Physicochemical and Engineering Aspects. 2005;**269**:119–124. DOI: 10.1016/j.colsurfa.2005.06.073

[58] Tan NPB, Lee CH, Li P. Green synthesis of smart metal/polymer nanocomposite particles and their tuneable catalytic activities. Polymer. 2016;**8**:105. DOI: 10.3990/polym804105

[59] Tian C, Mao B, Wang E, Kuang Z, Song Y, Wang C, Li S. Simple strategy for preparation of core colloids modified with metal nanoparticles. Journal of Physical Chemistry C. 2007;**111**:3651–3657. DOI: 10.1021/jp067077f

[60] Zelewsky AV, Barbosa L, Schlaper CW. Poly(ethyleneimines) as bronsted bases and as ligands for metal ions. Coordination Chemistry Reviews. 1993;**123**:229–246

[61] Mitric R, Burgel C, Burda J, Bonacic-Koutecky V, Fantucci R. Structural properties and reactivity of bimetallic silver-gold clusters. European Physical Journal D. 2003;**24**:41–44. DOI: 10.1140/epjde/e2003-00124-7

[62] Herrero E, Buller LJ, Abruna HD. Underpotential deposition at single crystal surfaces of Au, Pt, Ag and other materials. Chemical Reviews. 2001;**101**:1897–1930. DOI: 10.1021/cr9600363

[63] Wang D, Li Y. One-pot for Au-based hybrid magnetic nanostructures via a noble-metal-induced reduction process. Journal of the American Chemical Society. 2010;**132**:6280–6281. DOI: 10.1021/ja100845v

[64] Sato T, Ruch R. Stabilization of Colloidal Dispersion by Polymer Adsorption. New York: Marcel Dekker Inc.; 1980

[65] Marchetti B, Joseph Y, Bertagnolli H. Amine-capped gold nanoparticles: Reaction steps during the synthesis and the influence of the ligand on the particle size. Journal of Nanoparticle Research. 2011;**13**:3353–3362. DOI: 10.1007/s11051-011-0358-3

[66] Chen CC, Kuo PL, Cheng YC. Spherical aggregates composed of gold nanoparticles. Nanotechnology. 2009;**20**:055603. DOI: 10.1088/0957-4484/20/5/055603

[67] Liu Y, Fan Y, Yuan Y, Chen Y, Cheng F, Jiang SC. Amphiphilic hyperbranched copolymers bearing a hyperbranched core and a dendritic shell as novel stabilizers rendering gold nanoparticles with an unprecedentedly long lifetime in the catalytic reduction of 4-nitrophenol. Journal of Materials Chemistry. 2012;**22**:21173–21182. DOI: 10.1039/C2JM34445A

[68] Dey P, Blakey I, Thurecht KJ, Fredericks PM. Self-assembled hyperbranched polymer-gold nanoparticle hybrids: Understanding the effect of polymer overage on assembly size and SERS performance. Langmuir. 2013;**29**:525–533. DOI: 10.1021/la304034b

[69] Takagishi T, Okuda S, Kuroki N, Kozuka H. Binding of metal ions by polyethyleneimine and its derivatives. Journal of Polymer Science. 1985;**23**:2109–2116. DOI: 10.1002/pol.1985.170230804

[70] Horn D, Goethals EJ, editors. Polymeric Amines and Ammonium Salts. Oxford: Pergamon Press; **1980**. p. 333

[71] Wulff G, Dhal PK. Synthesis and Separations Using Functional Polymers. In: Sherrington DC, Hodge P, editors. Book Review: Zeolites, Crystal Growth, Polymers and Miscellanea. London: Wiley; 1988. p. 325

[72] Akamatsu K, Shimada M, Tsuruoka T, Nawafune H, Fujii S, Nakamura Y. Synthesis of pH-responsive nanocomposite microgels with size-controlled gold nanoparticles from ion-doped, lightly cross-linked poly(vinylpyridine). Langmuir. 2010;**26**:1254–1259. DOI: 10.1021/la902450c

[73] Ou JL, Chang CP, Ou KL, Tseng CC, Ling HW, Ger MD. Uniform polystyrene microsphere decorated with noble metal nanoparticles formed without using extra reducing agent. Colloids and Surfaces A: Physicochemical and Engineering Aspects. 2007;**305**:36–41. DOI: 10.1016/j.colsurfa.2007.04.038

[74] Haiss W, Thanh NTK, Aveyard J, Fernug DG. Determination of size and concentration of gold nanoparticles from UV-Vis spectra. Analytical Chemistry. 2007;**79**:4215–4221. DOI: 10.1021/ac0702084

[75] Leff DV, Brandt L, Heath JR. Synthesis and characterization of hydrophobic, organically-soluble gold nanocrystals functionalized with primary amines. Langmuir. 1996;**12**:4723–4730. DOI: 10.1021/la960445u

[76] Yang X, Shi M, Zhou R, Chen X, Chen H. Blending of $HAuCl_4$ and histidine in aqueous solution: A simple approach to the Au_{10}cluster. Nanoscale. 2011;**3**:2596–2601. DOI: 10.1039/C1NR10287G

[77] Zhang F, Srinivisan MP. Multilayered gold-nanoparticle/polyimide composite thin film through layer-by-layer assembly. Langmuir. 2007;**23**:10102–10108. DOI: 10.1021/la0635045

[78] Kumar A, Mandal S, Selvakannan PR, Pasricha R, Mandale AB, Sastry M. Investigation into the interaction between surface-bound alkylamines and gold nanoparticles. Langmuir. 2003;**16**:6277–6282. DOI: 10.1021/la034209c

[79] Manna A., Imae T, Aoi K, Okada M, Yogo T. Synthesis of dendrimer-passivated noble metal nanoparticles in a polar medium: Comparison of size between silver and gold particles. Chemistry of Materials. 2001;**13**:1674–1681. DOI: 10.1021/cm000416b

[80] Zhao C, Nie S, Tang M, Sun S. Polymeric pH-sensitive membranes—A review. Progress in Polymer Science. 2011;**36**:1499–1520. DOI: 10.1016/j.progpolymsci.2011.05.004

[81] Zhang P, Shao C, Zhang Z, Zhang M, Mu J, Guo Z, Liu Y. In situ assembly of well-dispersed Af nanoparticles (AgNPs) on electrospun carbon nanofibers (CNFs) for catalytic reduction of 4-nitrophenol. Nanoscale. 2011;**3**:3357–3363. DOI: 10.1039/C1NR10405E

[82] bin Saiman MI, Brett GL, Tiruvalam R, Forde MM, Sharples K, Thetford A, Jenkins RL, Dimitratos N, Lopez-Sanchez JA, Murphy DM, Bethell D, Willock DJ, Taylor SH, Knight DW, Kiely CJ, Hutchings GJ. Involvement of surface-bound radicals in the oxidation of toluene using supported Au-Pd nanoparticles. Angewandte Chemie-International Edition. 2012;**51**:5981–5985. DOI: 10.1002/anie.201201059

[83] Kesavan L, Tiruvalam R, Ab Rahim MH, bin Saiman MI, Enache DI, Jenkins RL, Dimitratos N, Lopez-Sanchez JA, Taylor SH, Knight DW, Kiely CJ, Hutchings GJ. Solvent-free oxidation of primary carbon-hydrogen bonds in toluene using Au-Pd alloy nanoparticles. Science. 2011;**331**:195–199. DOI: 10.1126/science.1198458

[84] Jirkovsky JS, Panas I, Ahlberg E, Halasa M, Romani S, Schiffrin DJ. Single atom hot-spots at Au-Pd nanoalloys for electrocatalytic H_2O_2 production. Journal of the American Chemical Society. 2011;**133**:19432–19441. DOI: 10.1021/ja206477z

[85] Garcia AG, Lopes PP, Gomes JF, Pires C, Ferreira EB, Lucena RGM, Gasparotto LHS, Tremiliosi-Filho G. Eco-friendly synthesis of bimetallic AuAg nanoparticles. New Journal of Chemistry. 2014, **38**,2865–2873. DOI:10.1039/c4nj00041b.

[86] Huang J, Vongehr S, Tang S, Lu H, Shen J, Meng X. Ag dendrite-based Au/Ag bimetallic nanostructures with strongly enhanced catalytic activity. Langmuir. 2009;**25**(19): 11890–11896. DOI: 10.1021/la9015383

[87] Zhang H, Haba M, Okumura M, Akita T, Hashimoto S, Toshima N. Novel formation of Ag/Au bimetallic nanoparticles by physical mixture of monometallic nanoparticles in dispersion and their application to catalysts for aerobic glucose oxidation. Langmuir. 2013;**29**:10330–10339. DOI: 10.1021/la401878g

IntechOpen